

Charged-Current Quasielastic (Anti)Neutrino Cross Sections on ^{12}C with Realistic Spectral Functions Including Meson-Exchange Contributions

**M.V. Ivanov¹, A.N. Antonov¹, G.D. Megias², J.A. Caballero²,
M.B. Barbaro³, J.E. Amaro⁴, I. Ruiz Simo⁴, T.W. Donnelly⁵,
J.M. Udías⁶**

¹Institute for Nuclear Research and Nuclear Energy, Bulgarian Academy of Sciences, Sofia 1784, Bulgaria

²Departamento de Física Atómica, Molecular y Nuclear, Universidad de Sevilla, 41080 Sevilla, Spain

³Dipartimento di Fisica, Università di Torino and INFN, Sezione di Torino, Via P. Giuria 1, 10125 Torino, Italy

⁴Departamento de Física Atómica, Molecular y Nuclear, and Instituto de Física Teórica y Computacional Carlos I, Universidad de Granada, Granada 18071, Spain

⁵Center for Theoretical Physics, Laboratory for Nuclear Science and Department of Physics, Massachusetts Institute of Technology, Cambridge, Massachusetts 02139, USA

⁶Grupo de Física Nuclear, Departamento de Estructura de la Materia, Física Aplicada y Electrónica and UPARCOS, Universidad Complutense de Madrid, CEI Moncloa, 28040 Madrid, Spain

Abstract. A detailed study of charged current quasielastic (anti)neutrino scattering cross sections on a ^{12}C target with no pions in the final state is presented. The initial nucleus is described by means of a realistic spectral function $S(p, \mathcal{E})$ in which nucleon-nucleon correlations are implemented by using natural orbitals through the Jastrow method. The roles played by these correlations and by final-state interactions are analyzed and discussed. The model also includes the contribution of weak two-body currents in the two-particle two-hole sector, evaluated within a fully relativistic Fermi gas. The theoretical predictions are compared with a large set of experimental data by the MiniBooNE, MINER ν A and T2K experiments. Good agreement with experimental data is found over the whole range of neutrino energies. The results are also in global good agreement with the predictions of the superscaling approach, which is based on the analysis of electron-nucleus scattering data, with only a few differences seen at specific kinematics.

1 Introduction

Having a good understanding of neutrino properties is presently one of the highest priorities in fundamental physics, explaining why considerable effort has been expended in recent years by a large number of researchers. Most of the recent (MiniBooNE, T2K, MINER ν A, NO ν A) and future (DUNE, HyperK) long baseline neutrino experiments make use of complex nuclear targets. Hence, precision measurement of neutrino oscillation parameters and the charge-parity (CP) violation phase requires one to have excellent control over medium effects in neutrino-nucleus scattering. In fact, nuclear modeling has become the main issue in providing neutrino properties with high accuracy. A detailed report on the study of neutrino-nucleus cross sections is presented in the NuSTEC White Paper [1].

The aim of the present paper (see also Ref. [2]) is to continue our work from Ref. [3] using the results obtained in Ref. [4] for a realistic spectral function $S(p, \mathcal{E})$ instead of the phenomenological superscaling approximation (SuSA) approach. The spectral function from our previous work [3] will be applied to analysis of CCQE (anti)neutrino cross sections on a ^{12}C target measured by the MiniBooNE [5, 6], MINER ν A [7, 8] and T2K [9] experiments. The new aspect of the present calculation concerns the treatment of 2p-2h excitations. In this work we include the fully relativistic weak (with vector and axial components) charged meson-exchange currents, in both longitudinal and transverse channels. These have been evaluated in [10–12] from an exact microscopic calculation, where the two-body current is the sum of seagull, pion-in-flight, pion-pole, and Δ -pole operators and the basis wave functions are noninteracting Dirac spinors.

2 General Formalism

2.1 Expression for the cross sections

The CC (anti)neutrino-nucleus inclusive cross section in the target laboratory frame can be written in the form (see [13, 14] for details)

$$\left[\frac{d^2\sigma}{d\Omega dk'} \right]_{\chi} = \sigma_0 \mathcal{F}_{\chi}^2, \quad (1)$$

where $\chi = +$ for neutrino-induced reactions (in the QE case, $\nu_{\ell} + n \rightarrow \ell^{-} + p$, where $\ell = e, \mu, \tau$) and $\chi = -$ for antineutrino-induced reactions (in the QE case, $\bar{\nu}_{\ell} + p \rightarrow \ell^{+} + n$). The function \mathcal{F}_{χ}^2 in Eq. (1) depends on the nuclear structure and is presented as a generalized Rosenbluth decomposition [13] containing leptonic kinematical factors, V_K , and five nuclear response functions, R_K , namely VV and AA charge-charge (CC), charge-longitudinal (CL), longitudinal-longitudinal (LL) and transverse (T) contributions, and VA transverse (T') contributions, where $V(A)$ denotes vector(axial-vector) current matrix elements. These are specific components of the nuclear tensor $W^{\mu\nu}$ in the

QE region and can be expressed in terms of the superscaling function $f(\psi)$ (see [13] for explicit expressions).

2.2 Models: HO+FSI, NO+FSI, and SuSAv2

In most neutrino experiments the interaction of the neutrino occurs with nucleons bound in nuclei. The analyses of such processes within different methods involve various effects such as nucleon-nucleon (NN) correlations, the final state interactions (FSI), possible modifications of the nucleon properties inside the nuclear medium and others. These effects, however, cannot be presently accounted for in an unambiguous and precise way, and what is very important, in most cases they are highly model-dependent. A possible way to avoid the model-dependencies is to use the nuclear response to other leptonic probes, such as electrons, under similar conditions to the neutrino experiments. The SuSA approach follows this general trend. The analyses of superscaling phenomena observed in electron scattering on nuclei have led to the use of the scaling function directly extracted from (e, e') data to predict (anti)neutrino-nucleus cross sections [13], just avoiding the usage of a particular nuclear structure model. A “superscaling function” $f(\psi)$ has been extracted from the data by factoring out the single-nucleon content of the double-differential cross section and plotting the remaining nuclear response versus a scaling variable $\psi(q, \omega)$ (q and ω being the momentum transfer and transferred energy, respectively). For high enough values of the momentum transfer (roughly $q > 400$ MeV) the explicit dependence of $f(\psi)$ on q is very weak at transferred energies below the quasielastic peak (scaling of the first kind). Scaling of second kind (*i.e.* no dependence of $f(\psi)$ on the mass number A) turns out to be excellent in the same region. The term “superscaling” means the occurrence of both first and second types of scaling.

In this work we consider three different theoretical calculations. Two of them, denoted as HO (harmonic oscillator) and NO (natural orbitals), make use of a spectral function $S(p, \mathcal{E})$, p being the momentum of the bound nucleon and \mathcal{E} the excitation energy of the residual nucleus, coinciding with the missing energy E_m up to a constant offset [15]. The area of analyses of the scaling function, the spectral function, and their connection (see, *e.g.*, Refs. [4, 16]) provides insight into the validity of the mean-field approximation (MFA) and the role of the NN correlations, as well as into the effects of FSI. Though in the MFA it is possible, in principle, to obtain the contributions of different shells to $S(p, \mathcal{E})$ and $n(p)$ for each single-particle state, owing to the residual interactions the hole states are not eigenstates of the residual nucleus but are mixtures of several single-particle states. The latter leads to the spreading of the shell structure and requires studies of the spectral function using theoretical methods going beyond the MFA to describe successfully the relevant experiments. In Ref. [4] a realistic spectral function $S(p, \mathcal{E})$ has been constructed that is in agreement with the scaling function $f(\psi)$ obtained from the (e, e') data. For this purpose effects beyond MFA have been considered. The procedure included (i)

the account for effects of a finite energy spread and (ii) the account for NN correlation effects considering single-particle momentum distributions $n_i(p)$ [that are components of $S(p, \mathcal{E})$] beyond the MFA, such as those related to the usage of natural orbitals (NO's) [17] for the single-particle wave functions and occupation numbers within methods in which short-range NN correlations are included. For the latter the Jastrow correlation method [18] has been considered. Also, in Ref. [4] FSI were accounted for using complex optical potential that has given a spectral function $S(p, \mathcal{E})$, leading to asymmetric scaling function in accordance with the experimental analysis, thus showing the essential role of the FSI in the description of electron scattering reactions.

In Figure 1 of Ref. [3] the results for the superscaling function $f(\psi)$ within the HO+FSI and NO+FSI models are presented. Accounting for FSI leads to a redistribution of the strength, with lower values of the scaling function at the maximum and an asymmetric shape around the peak position, *viz.*, when $\psi = 0$. Also, we see that the asymmetry in the superscaling function gets larger by using the Lorentzian function for the energy dependence of the spectral function than by using the Gaussian function [3, 4]. The two spectral function models, including FSI, clearly give a much more realistic representation of the data than the relativistic Fermi gas.

The third model, SuSAv2, that is an improved version of the superscaling prescription, called SuSAv2 [19], has been developed by incorporating relativistic mean field (RMF) effects [20–22] in the longitudinal and transverse nuclear responses, as well as in the isovector and isoscalar channels. This is of great interest in order to describe CC neutrino reactions that are purely isovector. Note that in this approach the enhancement of the transverse nuclear response emerges naturally from the RMF theory as a genuine relativistic effect.

The detailed description of the SuSAv2 model can be found in [19, 23, 24]. Here we just mention that it has been validated against all existing (e, e') data sets on ^{12}C , yielding excellent agreement over the full range of kinematics spanned by experiments, except for the very low energy and momentum transfers, where all approaches based on impulse approximation (IA) are bound to fail. Furthermore, the success of the model depends on the inclusion of effects associated with two-body electroweak currents, which will be briefly discussed in the next Section.

2.3 2p-2h MEC contributions

Ingredients beyond the impulse approximation (IA), namely 2p-2h MEC effects, are essential in order to explain the neutrino-nucleus cross sections of interest for neutrino oscillation experiments [1, 24–28]. In particular, 2p-2h MEC effects produce an important contribution in the “dip” region between the QE and Δ peaks, giving rise to a significant enhancement of the impulse approximation responses in the case of inclusive electron- and neutrino-nucleus scattering processes. In this work we make use of the 2p-2h MEC model developed in [11], which is an extension to the weak sector of the seminal papers [29–31] for the

electromagnetic case. The calculation is entirely based on the RFG model, and it incorporates the explicit evaluation of the five response function involved in inclusive neutrino scattering. The MEC model includes one-pion-exchange diagrams derived from the weak pion production model of [32]. This is at variance with the various scaling approaches that are largely based on electron scattering phenomenology, although also inspired in some cases by the RMF predictions.

Following previous works [23, 24, 33, 34], here we make use of a general parametrization of the MEC responses that significantly reduces the computational time. Its functional form for the cases of ^{12}C and ^{16}O is given in [23, 24, 35], and its validity has been clearly substantiated by comparing its predictions with the complete relativistic calculation.

3 Analysis of results

In this section we show the predictions of the two spectral function approaches previously described, HO and NO, both including FSI and 2p–2h MEC. We compare the results with data from three different experiments: MiniBooNE, MINER ν A and T2K. Our study is restricted to the QE-like regime where the impulse approximation in addition to the effects linked to the 2p–2h meson-exchange currents play the major role. We follow closely the general analysis presented in [24] for the case of the superscaling approach. Hence, for reference, we compare our new theoretical predictions with the results corresponding to the SuSAv2-MEC model.

The predicted ν_μ and $\bar{\nu}_\mu$ fluxes at the MiniBooNE [36], MINER ν A [37] and T2K [38] detectors and corresponding mean energies are compared in Figure 1. Φ_{tot} is the total integrated ν_μ ($\bar{\nu}_\mu$) flux factor: $\Phi_{\text{tot}} = \int \Phi(\varepsilon) d\varepsilon$, where ε is in-

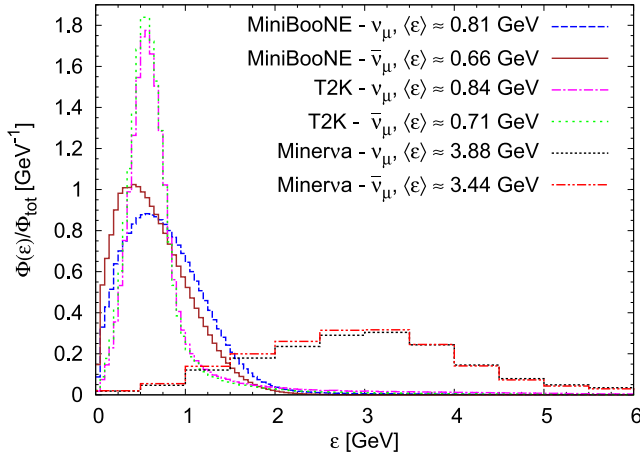


Figure 1. The predicted ν_μ ($\bar{\nu}_\mu$) fluxes at the MiniBooNE [36], MINER ν A [37] and T2K [38] detectors and corresponding mean energies.

cident beam energy. As observed, the neutrino and antineutrino mean energies corresponding to MiniBooNE and T2K experiments are rather similar, although the T2K energy flux shows a much narrower distribution. This explains the different role played by 2p-2h MEC effects in the two cases, these being larger for MiniBooNE (see [24] and results in next sections). On the contrary, the MINER ν A energy flux is much more extended to higher energies, with an average value close to 3.5 – 4.0 GeV.

3.1 MiniBooNE

In Figure 2 results are presented for the MiniBooNE flux averaged CCQE ν_μ - ^{12}C ($\bar{\nu}_\mu$ - ^{12}C) single differential cross section per nucleon as a function of the muon kinetic energy [left panels – (a) and (c)] and of the muon scattering angle [right panels – (b) and (d)]. The top panels [(a) and (b)] correspond to neutrino cross sections and the bottom [(c) and (d)] ones to antineutrino reactions. Theoretical predictions including both the QE and the 2p-2h MEC contributions are in good accord with the data. With regard to the comparison between the different models, we observe that HO+FSI and NO+FSI provide very close responses in all kinematical situations for neutrinos and antineutrinos: the inclusive cross section is not sensitive to the details of the spectral function. HO+FSI and NO+FSI

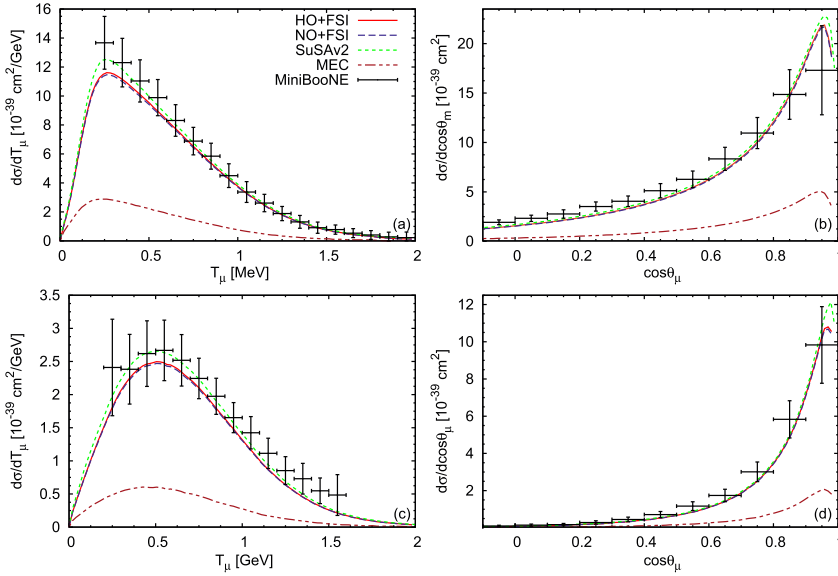


Figure 2. MiniBooNE flux-averaged CCQE ν_μ - ^{12}C ($\bar{\nu}_\mu$ - ^{12}C) differential cross section per nucleon as a function of the muon scattering angle [left panels – (a) and (c)] and of the muon kinetic energy [right panels – (b) and (d)]. The top panels [(a) and (b)] correspond to neutrino cross sections and the bottom [(c) and (d)] ones to antineutrino reactions. The data are from [5, 6].

lead to almost identical cross sections that differ from the SuSAv2 prediction by less than $\sim 5\% - 7\%$ at the maximum. The important contribution linked to the 2p-2h MEC (of the order of $\sim 20\% - 25\%$ of the total response) is clearly seen to be essential in order to describe the data. More results can be found in Ref. [2].

3.2 T2K

In Figure 3 we present the flux-averaged double differential cross sections corresponding to the T2K experiment [9]. The graphs are plotted against the muon momentum, and each panel corresponds to a bin in the scattering angle. As in the previous case, we show results obtained within the SuSAv2, HO+FSI, and NO+FSI approaches including MEC and also the separate contributions of the 2p-2h MEC. As already pointed out in [24], the narrower T2K flux, sharply peaked at about 0.7 GeV (see Figure 1), is the reason of the smaller contribution provided by the 2p-2h MEC (of the order of $\sim 10\%$) as compared with the Mini-BooNE results: in fact, the main contribution for the 2p-2h response comes from momentum transfers $q \sim 500$ MeV, which are less important at T2K kinematics. Concerning the theoretical predictions, the two SF models produce almost identical cross sections that deviate from SuSAv2, particularly at very forward scattering (right-bottom panel).

In the particular case of the most forward scattering kinematics (bottom panel on the right), notice that SuSAv2 cross section at the maximum exceeds SF+FSI results by $\sim 30\% - 35\%$. However, the large error bands shown by T2K data do not allow us to discriminate between the different models, *i.e.*, neither between pure QE calculations nor global QE+2p-2h MEC results. Furthermore, notice that the cross section reaches an almost constant value, different from zero, as p_μ increases. This is in contrast with all remaining situations explored in the previous figures.

3.3 MINER ν A

In Figure 4 we show the double differential cross section of muonic antineutrino on hydrocarbon as a function of the transverse (with respect to the antineutrino beam) momentum of the outgoing muon, in bins of the muon longitudinal momentum. As shown, the spread in the results ascribed to the three models used is small, of the order of $\sim 5\% - 6\%$ at the maximum. On the other hand, we note the excellent agreement between the theory and data once 2p-2h MEC effects ($\sim 20\% - 30\%$ at the maximum) are included. This significant contribution of the 2p-2h MEC effects is consistent with the results observed for MiniBooNE in spite of the very different muon antineutrino energy flux in the two experiments.

4 Conclusions

This work extends our previous studies of CCQE neutrino-nucleus scattering processes that are of interest for neutrino (antineutrino) oscillation experiments.

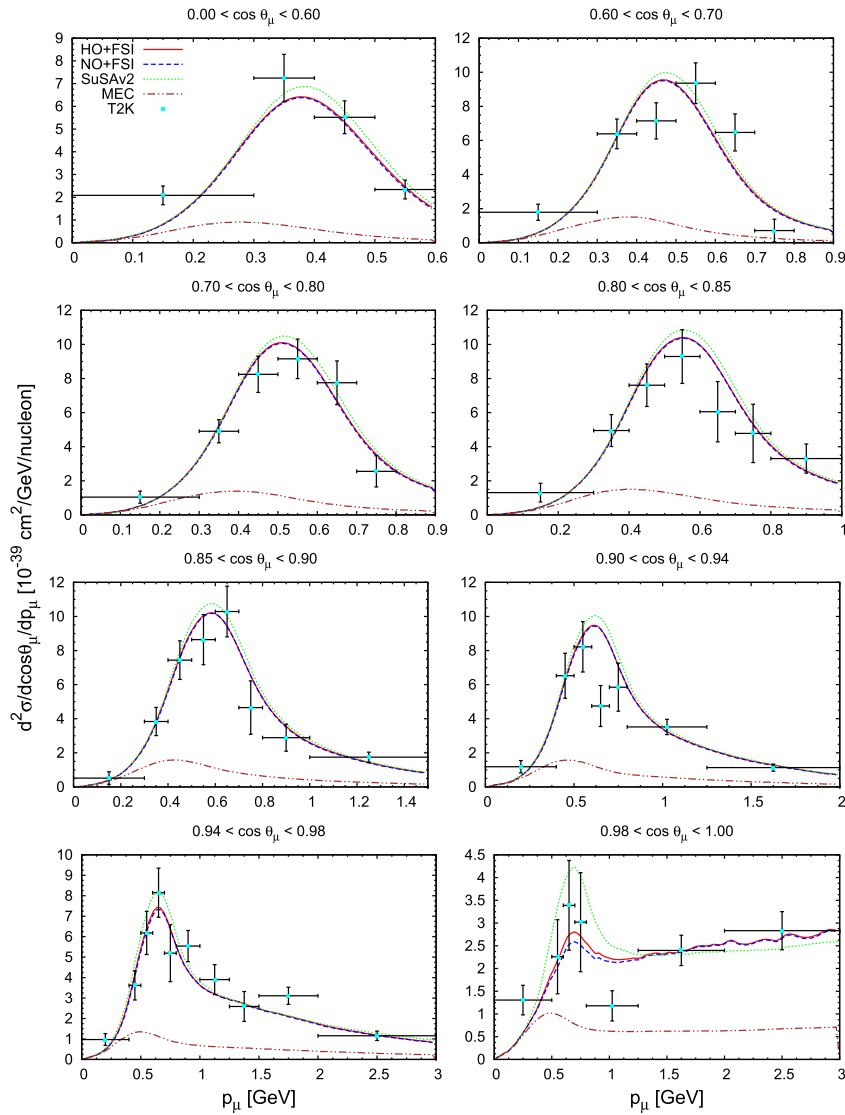


Figure 3. T2K flux-folded double differential cross section per target nucleon for the ν_μ CCQE process on ^{12}C displayed versus the μ^- momentum p_μ for various bins of $\cos\theta_\mu$ obtained within the SuSAv2, HO+FSI, and NO+FSI approaches including MEC. MEC results are shown also separately. The data are from [9].

Here we focus on models based on the use of two spectral functions, one of them including NN short-range correlations through the Jastrow method and, for a comparison, another without them. Effects of final-state interactions are

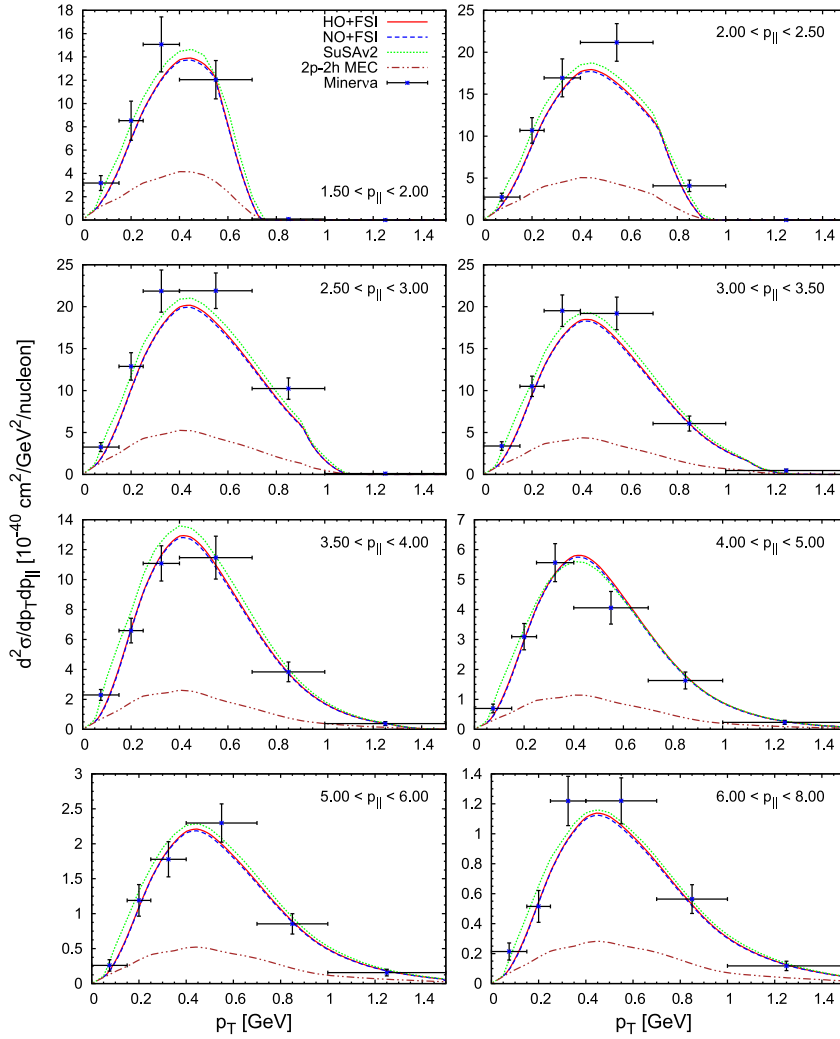


Figure 4. The MINER ν A “QE-like” double differential cross sections for $\bar{\nu}_\mu$ scattering on hydrocarbon versus the muon transverse momentum, in bins of the muon longitudinal momentum (in GeV). The data are from Ref. [7].

also incorporated by using an optical potential. These calculations, based on the impulse approximation, are complemented with the contributions given by two-body weak meson exchange currents, giving rise to two-particle two-hole excitations. The model is applied to three different experiments: MiniBooNE, MINER ν A, and T2K.

These new predictions are compared with the systematic analysis presented in [24] based on the SuSAv2+MEC approach. We find that the spectral function based models (HO+FSI, NO+FSI) lead to results that are very close to the SuSAv2-MEC predictions. Only at the most forward and most backward angles do the differences become larger, being at most of the order of $\sim 10\% - 12\%$. This is in contrast with the contribution ascribed to the 2p-2h MEC effects that can be even larger than $\sim 30\% - 35\%$ compared with the pure QE responses. This proves without ambiguity the essential role played by 2p-2h MEC in providing a successful description of neutrino (antineutrino)-nucleus scattering data for different experiments and a very wide range of kinematical situations.

An interesting outcome of the present study is that the results obtained with the NO spectral function, which accounts for NN short-range Jastrow correlations, are very similar to those obtained with the uncorrelated HO spectral function, thus indicating that the role played by this type of correlations is very minor for the observables analyzed in this study. The results in this work can be considered as a test of the reliability of the present spectral function based models. They compare extremely well with the SuSAv2 approach, based on the phenomenology of electron scattering data, although they fail in reproducing neutrino (antineutrino) scattering data unless ingredients beyond the impulse approximation are incorporated. The present study gives us confidence in extending the use of these models to other processes, such as semi-inclusive $CC\nu$ reactions and neutral current processes.

Acknowledgements

This work was partially supported by the Bulgarian National Science Fund under Contracts Nos. KP-06-N38/1, DNTS/Russia 01/3, by the Russian Foundation for Basic Research grant No. 17-52-18057-bolg-a, by the Spanish Ministerio de Economía y Competitividad and ERDF (European Regional Development Fund) under contracts FIS2014-59386-P, FIS2014-53448-C2-1, FIS2017-88410-P, FIS2017-85053-C2-1-P, FPA2015-65035-P, by the Junta de Andalucía (grants No. FQM-225, FQM160), by the INFN under project MANYBODY, by the University of Turin under contract BARM-RILO-17, and part (TWD) by the U.S. Department of Energy under cooperative agreement DE-FC02-94ER40818. GDM acknowledges support from a Junta de Andalucía fellowship (FQM7632, Proyecto de Excelencia 2011). MBB acknowledges support from the “Emilie du Châtelet” programme of the P2IO LabEx (ANR-10-LABX-0038).

References

- [1] L. Alvarez-Ruso *et al.*, *Prog. Part. Nucl. Phys.* **100** (2018) 1.
- [2] M. V. Ivanov *et al.*, *Phys. Rev. C* **99** (2019) 014610.
- [3] M. V. Ivanov *et al.*, *Phys. Rev. C* **89** (2014) 014607.
- [4] A. N. Antonov *et al.*, *Phys. Rev. C* **83** (2011) 045504.

- [5] A. A. Aguilar-Arevalo *et al.*, (MiniBooNE Collaboration), *Phys. Rev. D* **81** (2010) 092005.
- [6] A. A. Aguilar-Arevalo *et al.*, (MiniBooNE Collaboration), *Phys. Rev. D* **88** (2013) 032001.
- [7] C. E. Patrick *et al.*, (MINER ν A Collaboration), *Phys. Rev. D* **97** (2018) 052002.
- [8] D. Ruterbories *et al.*, (MINER ν A Collaboration), *Phys. Rev. D* **99** (2019) 012004.
- [9] K. Abe *et al.*, (T2K Collaboration), *Phys. Rev. D* **93** (2016) 112012.
- [10] I. R. Simo *et al.*, *Phys. Rev. D* **90** (2014) 033012.
- [11] I. Ruiz Simo *et al.*, *J. Phys.* **G44** (2017) 065105.
- [12] I. R. Simo *et al.*, *Phys. Rev. C* **94** (2016) 054610.
- [13] J. E. Amaro *et al.*, *Phys. Rev. C* **71** (2005) 015501.
- [14] D. B. Day *et al.*, *Annu. Rev. Nucl. Part. Sci.* **40** (1990) 357.
- [15] M. Barbaro *et al.*, *Nuclear Physics A* **643** (1998) 137.
- [16] J. A. Caballero *et al.*, *Phys. Rev. C* **81** (2010) 055502.
- [17] P.-O. Löwdin, *Phys. Rev.* **97** (1955) 1474.
- [18] M. V. Stoitsov, A. N. Antonov, and S. S. Dimitrova, *Phys. Rev. C* **48** (1993) 74.
- [19] R. González-Jiménez *et al.*, *Phys. Rev. C* **90** (2014) 035501.
- [20] J. A. Caballero *et al.*, *Phys. Rev. Lett.* **95** (2005) 252502.
- [21] J. A. Caballero, *Phys. Rev. C* **74** (2006) 015502.
- [22] J. Caballero *et al.*, *Physics Letters B* **653** (2007) 366.
- [23] G. D. Megias *et al.*, *Phys. Rev. D* **94** (2016) 013012.
- [24] G. D. Megias *et al.*, *Phys. Rev. D* **94** (2016) 093004.
- [25] J. E. Amaro *et al.*, *Phys. Lett. B* **696** (2011) 151.
- [26] J. Nieves *et al.*, *Physics Letters B* **707** (2012) 72.
- [27] O. Lalakulich *et al.*, *Phys. Rev. C* **86** (2012) 014614.
- [28] T. Katori and M. Martini, *J. Phys. G: Nucl. Part. Phys.* **45** (2018) 013001.
- [29] J. W. Van Orden and T. W. Donnelly, *Annals Phys.* **131** (1981) 451.
- [30] A. De Pace *et al.*, *Nucl. Phys.* **A726** (2003) 303.
- [31] J. E. Amaro *et al.*, *Phys. Rev. C* **82** (2010) 044601.
- [32] E. Hernández, J. Nieves, and M. Valverde, *Phys. Rev. D* **76** (2007) 033005.
- [33] G. D. Megias *et al.*, *Phys. Rev. D* **91** (2015) 073004.
- [34] M. V. Ivanov *et al.*, *J. Phys. G: Nucl. Part. Phys.* **43** (2016) 045101.
- [35] G. D. Megias *et al.*, *J. Phys. G: Nucl. Part. Phys.* **46** (2018) 015104.
- [36] A. A. Aguilar-Arevalo *et al.*, (MiniBooNE Collaboration), *Phys. Rev. D* **79** (2009) 072002.
- [37] L. Aliaga *et al.*, (MINER ν A Collaboration), *Phys. Rev. D* **94** (2016) 092005.
- [38] K. Abe *et al.*, (T2K Collaboration), *Phys. Rev. D* **87** (2013) 012001.